

Up-Grade Recycling of Metallic Cutting Chips by Consolidation under Severe Plastic Deformation

H. Toda, T. Kobayashi, J. Sawamura

Department of Production Systems Engineering, Toyohashi University of Technology,
1-1, Hibarigaoka, Tempaku, Toyohashi, 441-8580, Japan

Keywords: cutting chips, up-grade recycling, severe plastic deformation, consolidation, composite, swaging.

Abstract

Cutting chip may be identified utilizable due to highly accumulated strain (typically 2 – 3) during cutting. In this study, aluminium chips are consolidated by cold severe plastic deformation so that their highly deformed microstructure is utilized for strengthening. Consolidated chips exhibit much finer microstructure at the same applied strain. In addition, incorporating secondary phases by adding the cutting chip of a dissimilar metal is also proposed for further strengthening. To predict the attainable strength, the Eshelby model is employed. The present method is identified to realize superior strength which is about 2.3 times that of the aluminium before cutting.

1. Introduction

Cutting chip is, generally, separated from cutting oil and then remelted for recycling solely as raw materials. Materials recycled in this way may be identified to have inferior properties to primary ingots. For example, in the case of aluminium alloys, recycled aluminium always exhibits higher Fe content because aluminium components are usually used being assembled with steel parts. Hence, corrosion resistance and mechanical properties are significantly degraded by the existence of Fe-bearing intermetallics in its microstructure [1]. In terms of microstructures, however, the cutting chip may be identified utilizable due to highly-accumulated strain (usually 2 – 3 in plastic strain) during cutting. In this study, aluminium chips are consolidated by cold severe plastic deformation so that their highly deformed microstructure is preserved in a consolidated material for strengthening. Also, heavily deformed *in-situ* composite technique may be available for the further strengthening of the chips as it has been reported to exhibit anomalous increase in tensile strength with heavy deformation [2]. A steel or a copper cutting chip is used as the second phase to be incorporated into the aluminium cutting chips. To predict the attainable maximum strength from the limited amount of experimental data within the present study, the Eshelby equivalent inclusion model is employed.

2. Experimental

According to the preliminary investigation, cutting procedure and its condition are determined to be milling with relatively small cutting depth (0.1mm) and the highest cutting speed (16.7mm/s). A 6061-T651 aluminium alloy was used to prepare aluminium cutting chips. An IF steel (0.0017%C-0.006%Si-0.13%Mn-0.012%P-0.006%S-0.029%Al-

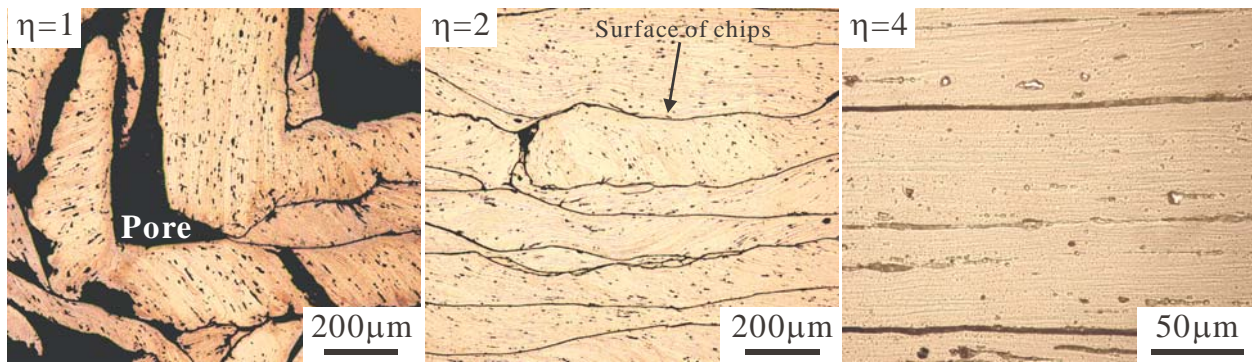


Figure 1: Optical micrographs of longitudinal cross sections at various drawing strain levels in AL_c.

0.018%Ti-0.013%Nb) and a 99.9% copper are used as second phases. The volume fractions of the second phase were 0 and 20 % in both of the cases. These samples are distinguished as AL_c, AL-FE and AL-CU, respectively. Another monolithic aluminium (AL_c-5%AL_p) was prepared in which 5% of 6061 powder was added to eliminate interfacial debonding among former cutting chip surface. The subscripts, c and p denote chip and particle, respectively.

The cutting chip mixtures were mixed by a V-type mixer for 5.4 ks. The cutting chips were then uni-axially pressed under a pressure of 224 MPa using a pressing machine. Powder compacts of about 20 mm both in diameter and length were then filled in 21.6 mm-o.d. copper tubes, and were then swaged to 1.5 mm in diameter. Apparent drawing strain defined by $\eta = \ln \frac{A_0}{A}$ (A_0 and A are cross-section areas before and after swaging) reaches

5.4 at this stage. The copper skin was removed by etching in HNO₃. All the processes including the packing were performed in room temperature air without using any special apparatus. 6061 alloy particles were consolidated and swaged in the same way. Also a bulk 6061 alloy was swaged to the same strain level. Both the materials were used for

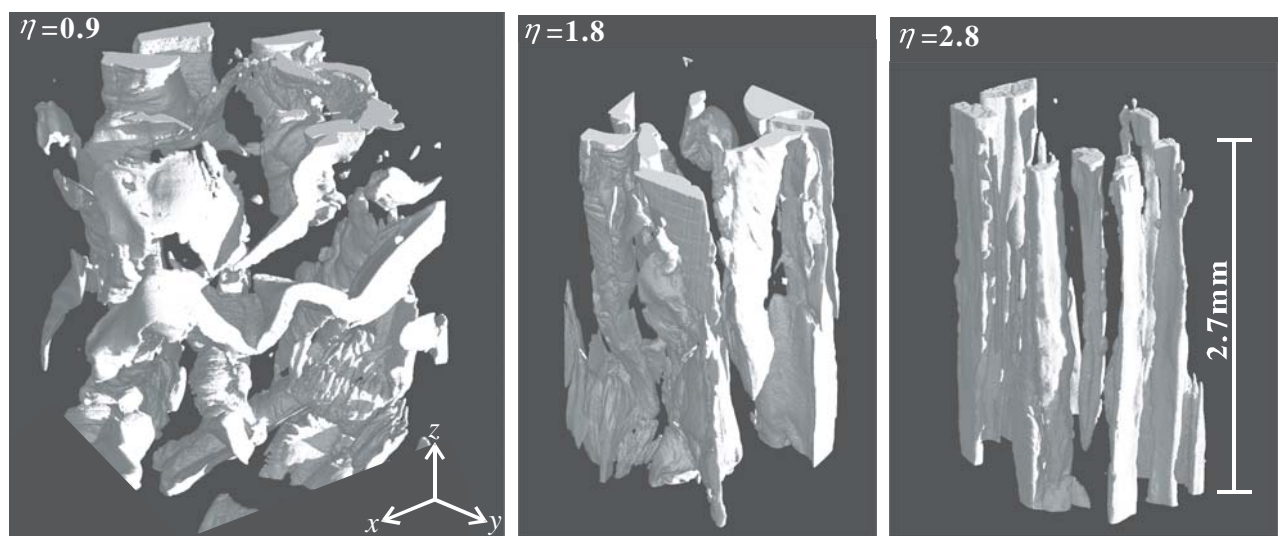


Figure 2: 3D perspective views of the iron phase extracted from tomographic volumes, representing shape change of the iron phase during swaging in AL-FE.

comparison purpose and distinguished as AL_p and AL_b , respectively. Here, b denotes bulk.

X-ray-computed tomography was used to image the deformation behaviour of the second phases. A sealed tube operated at 98kV was used with a 1024X1024 cooled CCD. The projections captured were reconstructed with $2.73\mu\text{m}$ isotropic voxels using the FeldKamp corn-beam algorithm.

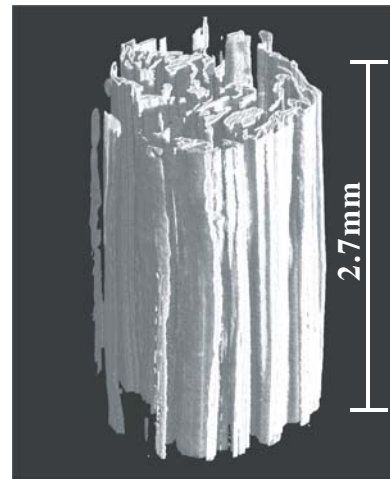


Figure 3: 3D perspective views of the iron fibers extracted from tomographic volumes which are captured at $\eta=5.4$ in AL-FE.

3. Results and Discussion

3.1 Microstructure

Figure 1 shows the optical micrographs of monolithic aluminium chips, AL_c , on longitudinal sections, which show how the microstructure was developing during the deformation process. Firstly bending and breakage of the chips occurred during the pressing. Porosity was however high at this stage as shown by the left photograph in Figure 1. Although the chips were uniaxially aligned in the subsequent swaging process, flow lines within each cutting chip were seen not to align so perfectly at such earlier stages. Complete consolidation was not achieved before the drawing strain of about 4.

Figure 2 shows 3D perspective views of AL-FE, in which the iron phase was extracted from tomographic volumes, representing shape change of the iron phase during swaging. The iron phase started to orient in the swaging direction at about $\eta=1.8$ then start splitting in the transverse direction at about $\eta=2.8$. Fig.3 is the similar volume rendered images at $\eta=5.4$. The iron cutting chips were transformed into filament-like shape at this stage

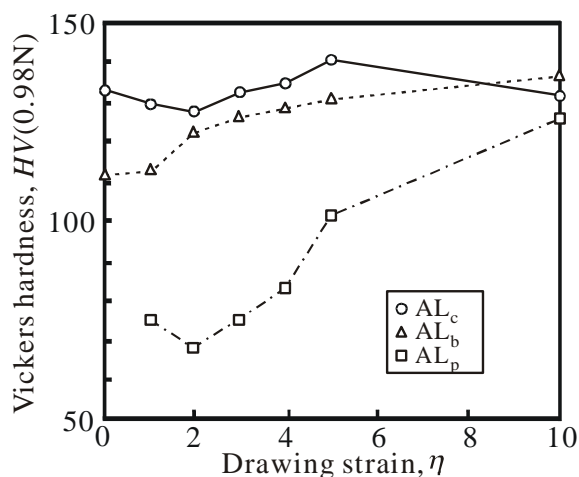


Figure 4: Vickers hardness as a function of drawing strain in AL.

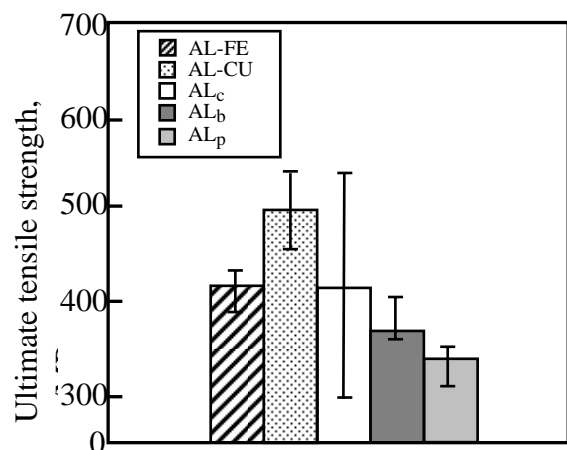


Figure 5: Ultimate tensile strengths as a function of drawing strain.

curling like a curtain in the transverse direction. The BCC crystals are known to develop an $\langle 110 \rangle$ fibre texture in which only two of the four $\langle 111 \rangle$ directions are oriented favourably to accommodate plastic strain parallel to the wire axis [3]. This mode produces plane strain

deformation of the BCC metal. The BCC phase may be forced to curl in order to maintain compatibility in displacement with a needle-like FCC phase which deforms in an axisymmetric way.

Figure 4 shows the variation in Vickers hardness as a function of drawing strain in AL. The hardness apparently decreases until the drawing strain reached 2 except the bulk material, which may be presumably due to the existence of pores. It is clearly advantageous that the hardness value of AL_c is always higher than that of AL_b by a specific amount during the initial drawing process (i.e. $\sim \eta = 5.4$). The hardness drop observed above $\eta = 5.4$ in AL_c is attributable to production defects as will be shown later. The Vickers hardness of the iron phase increased from 177 to 192 between η of 0 and 5.4, while that of the copper phase was almost constant around 100.

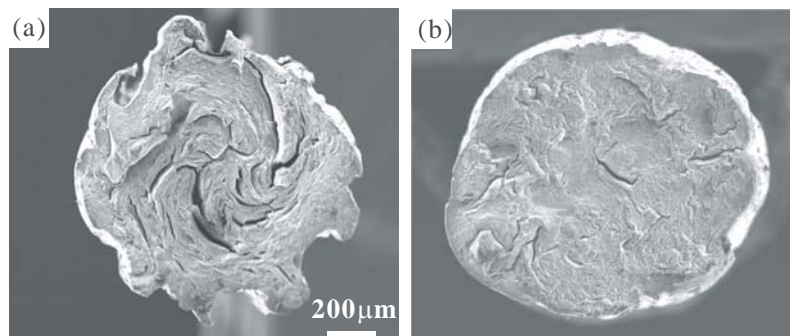


Figure 6: SEM micrographs of fracture surfaces after tensile tested at the drawing strain of 5.4. (a) AL_c and (b) AL-FE.

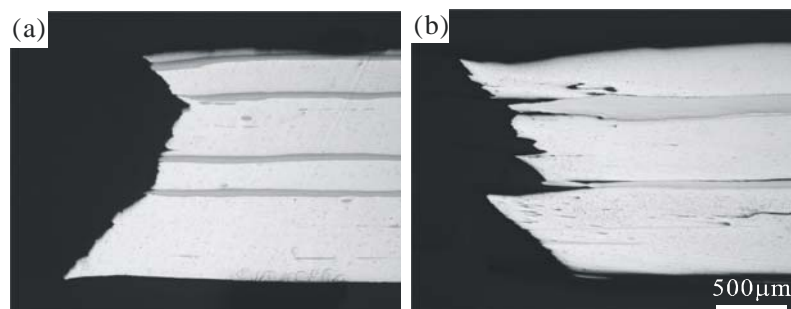


Figure 7: Optical micrographs of longitudinal cross sections including fracture surfaces. (a) AL-FE and (b) AL-CU.

3.2 Mechanical Properties.

Figure 5 shows ultimate tensile strength and its variations at $\eta = 5.4$. The significant variations in the tensile strength are characteristically observed in AL_c , suggesting that the possibility of containing the fatal fabrication defects determines its tensile strength. This can be clearly confirmed in Fig.6 (a) where fracture surface of AL_c was observed after the tensile test. It is clear that secondary cracking perpendicular to the fracture surface is extensively observed along spiral flow lines

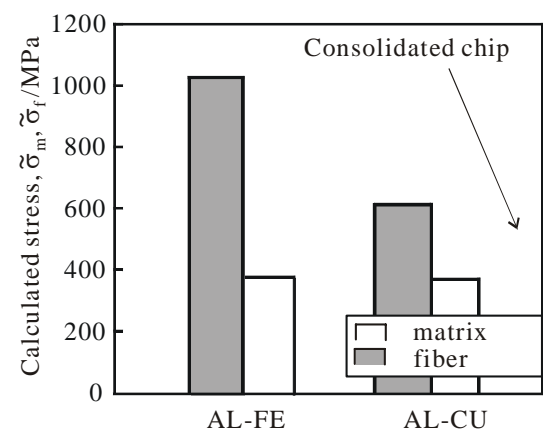


Figure 8: Estimated fiber and matrix stresses at composite fracture by the Eshelby equivalent inclusion method under the assumption of iso-strain condition.

formed during the swaging process. These secondary cracks were confirmed to be the former surface of cutting chips by a closer inspection. Remarkable surface roughness of AL_c means that interfacial sliding occurs even during swaging. It may be reasonable to expect the effective improvement of the tensile strength by eliminating such defects. When 5% of the 6061 powder is mixed with the 6061 cutting chips, the variation in tensile strength could be effectively suppressed. In the case of AL-FE and AL-CU, such significant scattering was not observed. As the previous study suggested [4], mutual constraint between the aluminium cutting chip and the second phases may be effective to break rigid oxide film on the former cutting chip surface. Note that the secondary cracks on fracture surface could not be eliminated completely even in AL-FE and AL-CU as shown in Fig.6 (b).

3.3 Prediction of the Attainable Strength in Composites

In order to estimate the maximum tensile strength which is attainable by incorporating secondary cutting chips, the Eshelby's equivalent inclusion method [5] was utilized. Equation (1) and (2), which express a fibre and a matrix stresses, were solved to estimate those stresses at composite fracture.

$$\tilde{\sigma}_f = \tilde{\sigma}_0 + \tilde{\sigma}_f^i = \tilde{C}_f(\tilde{\varepsilon}_0 + \tilde{\varepsilon} + \tilde{\varepsilon} - \tilde{\varepsilon}_f^p + \tilde{\varepsilon}_m^p) = \tilde{C}_m(\tilde{\varepsilon}_0 + \tilde{\varepsilon} + \tilde{\varepsilon} - \tilde{\varepsilon}^*) \quad (1)$$

$$\tilde{\sigma}_m = \tilde{\sigma}_0 + \tilde{\sigma}_m^i = \tilde{C}_m(\tilde{\varepsilon}_0 + \tilde{\varepsilon}) \quad (2)$$

where σ , ε and C are stress, strain and elastic constants, respectively. Subscripts 0, f and m denote external stress, fibre and matrix, respectively. Superscripts i and p denote internal stress and plastic strain, respectively. Strain in a monolithic aluminium alloy, $\tilde{\varepsilon}_0$, has the relation, $\tilde{\sigma}_0 = \tilde{C}_m \cdot \tilde{\varepsilon}_0$. Strain variation due to the existence of a second phase can be divided into an average, $\tilde{\varepsilon}$, and local variation, $\tilde{\varepsilon}$, where $\tilde{\varepsilon}$ has the relationship, $\tilde{\sigma}_m = \tilde{C}_m \cdot \tilde{\varepsilon}$. Since internal stresses are offset if summed over the whole material, $(1-f)\tilde{\sigma}_m^i + f\tilde{\sigma}_f^i = 0$ (f : volume fraction) holds. Unknown eigenstrain, $\tilde{\varepsilon}^*$ is related linearly to $\tilde{\varepsilon}$ through Eshelby tensor, \tilde{S} . On the basis of the observation of longitudinal cross section including a fracture surface, which is shown in Fig.7, iso-strain deformation between the matrix and the secondary phases were assumed. The assumption of iso-strain can be expressed as eq.(3) using eqs. (1) and (2). Finally, the matrix and fibre stresses are expressed as eqs.(4) and (5).

$$\tilde{\varepsilon}_0 + \tilde{\varepsilon} + \tilde{\varepsilon} - \tilde{\varepsilon}_f^p + \tilde{\varepsilon}_m^p = \tilde{\varepsilon}_0 + \tilde{\varepsilon} \quad (3)$$

$$\tilde{\sigma}_m = \tilde{C}_m[\tilde{C}_m^{-1} - f\{(1-f)\tilde{C}_m + f\tilde{C}_f\}^{-1}(\tilde{C}_f\tilde{C}_m^{-1} - \tilde{I})]\tilde{\sigma}_0 \quad (4)$$

$$\tilde{\sigma}_f = \tilde{C}_f[\tilde{C}_m^{-1} - f\{(1-f)\tilde{C}_m + f\tilde{C}_f\}^{-1}(\tilde{C}_f\tilde{C}_m^{-1} - \tilde{I})]\tilde{\sigma}_0 \quad (5)$$

Figure 8 shows the calculated matrix and fibre stresses, respectively. Comparing with the previous report [4], the fracture strength of a monolithic 6061 aluminium alloy which is produced from cutting chips is 41 – 67 % higher than that of the matrix stresses at composite fracture. This implies that even if much stronger cutting chip is incorporated as a reinforcement, the aluminium matrix can bear much higher stress, thereby increasing composite strength. The present method is identified to have a potential of realizing 713MPa (about 2.3 times that of the material before cutting) in the case of the present 6061 alloy / IF steel composite as shown in Table 1.

Table 1: Predicted maximum ultimate tensile strength in AL-FE.

Matrix strength	Maximum composite strength	Fiber stress at composite fracture
530MPa (AL_c)	713MPa (Prediction)	1440MPa (Prediction)

4. Conclusions

Aluminium chips were consolidated by cold severe plastic deformation so that their highly accumulated strain was utilized for strengthening. The aluminium chips have been successfully consolidated by a combination of pressing and swaging in room temperature air. The consolidated chips exhibited superior strength to a wrought alloy together with finer microstructure when compared at a same applied strain. In addition, incorporating secondary phases by adding the cutting chip of a dissimilar metal is also proposed for further strengthening. The iron cutting chips were transformed into thin filament-like shape curling like a curtain in the transverse direction. To predict the attainable maximum strength in this composite, the Eshelby equivalent inclusion model is employed. The present method is identified to realize superior strength which is about 2.3 times that of the aluminium before cutting. Overall, the utilization of the cutting chips was identified as a highly effective way of recycling such industrial waste by which materials with superior mechanical properties to original materials can be created by a combination of the conventional processes. This technique may be identified also available in a variety of alloy systems such as steel, cast iron, titanium, etc., including the creation of metal/glass, metal/ceramics and even metal/polymer composites by combining various waste chips.

Acknowledgements

The research was supported by the light metal educational foundation in Japan through grant-in-aid to TK and the Grant-in-aid for Scientific Research from JSPS through subject No. 14655256.

References

- [1] H.Toda and T.Kobayashi, Material Science Forum, 396-402, 1097-1102, 2002.
- [2] H. Toda and T. Kobayashi, Int. J. of Mater. Product Tech., SPM1, 427, 2001.
- [3] W.F.Hosford, Jr., Trans. Metall. Soc. AIME 230, 12, 1964.
- [4] H. Toda and T. Kobayashi, Materials Science Forum, (2004), in press.
- [5] J.D.Eshelby, Progress in Solid Mechanics 2, North-Holland, 89-140, 1961.